Tetrahedron Letters xxx (2015) xxx–xxx

Contents lists available at ScienceDirect

Tetrahedron Letters

journal homepage: www.elsevier.com/locate/tetlet

A C_{3v}-symmetric triphosphine ligand derived from trindane skeleton: synthesis, inclusion of C_{60}, and catalytic activity of its Pd complex

Dong Seob Lim [a], Suban K. Sahoo [a,b], Chan Sik Cho [a], Yang Kim [c], Heung-Jin Choi [a,*]

[a] Department of Applied Chemistry, Kyungpook National University, Daegu, 702-701, South Korea
[b] Department of Applied Chemistry, SV National Institute of Technology, Surat, Gujrat 395007, India
[c] Department of Chemistry & Advanced Materials, Kosin University, 194 Wachi-Ro, Yeongdo-gu, Busan 606-701, South Korea

ARTICLE INFO

Article history:
Received 16 July 2015
Revised 20 August 2015
Accepted 25 August 2015
Available online xxxx

Keywords:
Trisphosphine ligand
Suzuki–Miyaura cross-coupling
Inclusion complexation
C_{60}
^{31}P NMR

ABSTRACT

With the aim to design a multidentate C_{3v}-symmetric trindane-based trisphosphine ligand **3** for Suzuki–Miyaura cross-coupling of 3-bromothiophene with phenylboronic acid, we observed the ability of this ligand to form an inclusion complex with buckyball C_{60}. Along with its catalytic activity, the pyramidal inversion at phosphorous atoms of **3** and the formation of **3**@C_{60} were investigated by ^{1}H NMR, ^{31}P {^{1}H} NMR and DFT methods.

Phosphine ligands are well known in chemistry because of their fascinating coordination behavior with various transition metal ions and wide industrial applications as catalysts.[1,2]. The use of phosphines as supporting ligands for cross-coupling reactions generating carbon–carbon bonds, in particular the Pd-catalyzed Suzuki–Miyaura reaction of aryl halides with organoboron reagents for the synthesis of biaryls, is well known due to several advantages such as mild reaction conditions, high tolerance toward reactive functional groups, commercial availability of various boronic acids, and ease of separation of the products from the boron-containing byproducts.[3–6] These advantages have made Suzuki–Miyaura coupling (SMC) a reaction of choice in the large-scale synthesis of pharmaceutical compounds, fine chemicals, and polymers. Recent results with multidentate phosphines having a preorganized structure known to stabilize the palladium catalyst and also improved the catalytic activity.[7–9] The present work is an extension of this approach to catalyst improvement.

Moreover, the development of molecular clips having conjugated aromatic side arms with complementary cavity to wrap buckyballs like C_{60} through pi-pi interactions has gained an immense interest in the field of nanoscience and technology after the first experimental evidence of stable inclusion complex of C_{60} was reported in 2007.[10–13] As a part of our ongoing research on multifunctional ligands design using the rigid tripodal framework trindane,[14–16] herein, we introduced a novel C_{3v} symmetric trisphosphine ligand to enrich the ligand library of SMC reactions. Further, the ability to encapsulate C_{60} within the cavity formed by the trisphosphine of **3** was examined by NMR and DFT methods.

The synthesis of trisphosphine ligand **3** was presented in Scheme 1. The synthesis of starting compound **1**, that is, benzyl chloride derivative of trindane was carried out by following our reported method.[14] Because of the slow reactivity of the nucleophilic substitution reaction to get the intermediate compound **2**, the starting compound **1** was first heated at 100 °C for 30 min directly in neat ethyl diphenylphosphinite and then the mixture was refluxed in toluene for another 2 h. Further purification by column chromatography gave **2** in 95% yield. Reduction of **2** with $PhSiHCl_2$ in THF was carried out to afford the desired trisphosphine ligand **3** under nitrogen environment. It was observed that the alkyl phosphine product in THF sensitively reacted with oxygen upon contact with air and was oxidized back to phosphine oxide. Therefore, without any much exposure to the surrounding, the reaction solvent and volatile by-products were removed by vacuum distillation at high temperature and then vacuum-dried to get the desired trisphosphine **3** quantitatively.

The molecular structures of **2** and **3** were established by various spectroscopic data (^{1}H NMR, ^{13}C NMR, ^{31}P NMR, and HR-MS). From ^{1}H NMR, the appearance of two sets of doublets for **2** (δ 3.18 and 2.80 ppm, ^{2}J = 15.7 Hz) (Fig. S1a) and **3** (δ 3.15 and 2.77 ppm, ^{2}J = 15.8 Hz) due to the two diastereotopic benzylic protons of

* Corresponding author. Tel.: +82 53 950 5582; fax: +82 53 950 6594.
E-mail address: choihj@knu.ac.kr (H.-J. Choi).

http://dx.doi.org/10.1016/j.tetlet.2015.08.069
0040-4039/

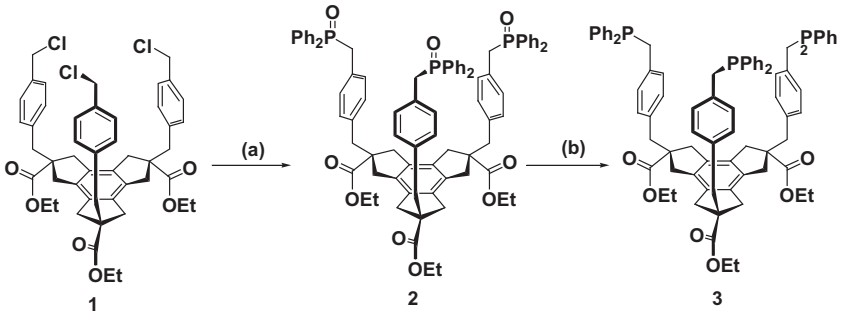

Scheme 1. Synthesis of trisphosphine ligand **3**. Reagents and conditions: (a) (i) Ph_2POEt, 100 °C, 30 min and (ii) toluene, reflux, 2 h; (b) $PhSiHCl_2$, THF, reflux, 18 h.

the trindane skeleton and the singlet for the methylene groups of benzyl groups at 2.95 and 2.90 ppm, respectively, confirmed the C_{3v}-symmetrical conformation of the trindane derivatives. In ^{31}P NMR, the phosphine oxide **2** and reduced phosphine **3** gave only one kind of singlet respectively at δ 31.2 and δ 4.7 ppm indicative of the structural purity of the compounds.

The trisphosphine ligand **3** along with the two commercial phosphines, that is, triphenylphosphine (**4**) and 1,2-bis(diphenylphosphino) (**5**) were applied as a ligand for the Pd-catalyzed Suzuki–Miyaura cross-coupling of 3-bromothiophene with phenylboronic acid (Table 1). The prolonged reaction time of 40 h was kept for all the three phosphines to evaluate the catalytic activity with their overall turnover. As summarized in Table 1, the Pd-catalyzed reaction with trisphosphine ligand **3** showed better activity on the cross-coupling reaction compared to monophosphine and diphosphine. The preorganized structure of **3** with multiphosphine groups along with the cooperative effect increases the catalytic activity.

In ^1H NMR of **3** (Fig. 1) recorded at room temperature, we observed a broad peak for the methylene group of the phosphine possibly due to the pyramidal inversion slower than the NMR time scale, instead well-defined all sharp peaks due to the corresponding phosphine oxide **2**. The broad singlet at 4.6 ppm of the methylene group of phosphine at 297 K was shifted upfield upon increasing the temperature due to the conformation rotation at phosphine without any significant changes in the overall C_{3v} symmetry of **3**. When the temperature increased to 323 K, the pyramidal inversion on phosphine is getting faster and therefore resulted a broad doublet at 3.5 ppm for the methylene protons coupled with phosphorous nuclei ($^2J_{HP}$ = 13 Hz). The possible pyramidal inversion of phosphine group of **3** was clearly identified in the ^{13}C NMR (Fig. S2). The peaks observed between 128 and 136 ppm of **3** were comparatively broad rather than the specific chemical shift owing to the presence of variety of molecular inversion conformers

Table 1
Palladium-catalyzed cross-coupling reaction of 3-bromothiophene (1 mmol) with phenylboronic acid (1.5 mmol) with phosphine ligands **3**, **4**, and **5**

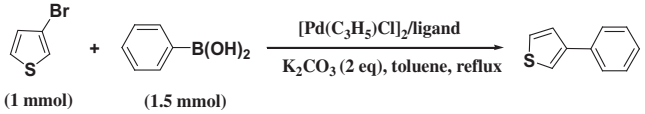

Entry	Pd catalyst (μmol)	Ligand (μmol)	Reaction time (h)	Yield* (%)
1	0.4	0	20	8
2	0.2	**5** (0.2)	40	15
3	0.2	**4** (0.4)	40	33
4	0.2	**3** (0.2)	40	86

* Reaction conditions: $[Pd(C_3H_5)Cl]_2$ as palladium catalyst in toluene (5 mL) at reflux, yields determined by gas chromatography.

at equilibrium compared to the phosphine oxide **2** (Fig. S1). The pyramidal inversion of phosphine also affects the chemical shift of the proton decoupled $^{31}P\{^1H\}$ NMR spectrum of **3** recorded at various temperatures (Fig. 2). Similar to the ^1H NMR observation, the phosphine peak at 4.7 ppm (297 K) was shifted upfield to −6 ppm (323 K) upon increasing the temperature. The broad singlet at various temperatures indicates that the symmetry of the molecule is maintained over a wide temperature.

The rigid C_{3v} symmetric trindane derived trisphosphine with multi-aromatic systems and preorganized cavity is expected to act as a tripodal molecular clip to encapsulate fullerenes like C_{60}. To get a preliminary information on the inclusion complexation behavior of **3**, a saturated solution of C_{60} in $CDCl_3$ (solubility of C_{60} in chloroform: 0.16 mg/mL[17]) was treated with **3** (10 mM), and the $^{31}P\{^1H\}$ NMR spectrum was recorded at different temperatures (Fig. 3). At 297 K, the free ligand **3** showed a small broad peak at 4.7 ppm. In the presence of C_{60}, a new sharp multiplet at 42.5 ppm appeared due to the formation of an inclusion complex with C_{60} through CH–π/π–π interactions. With the rise in temperature from 297 K to 323 K, the peak characterized for the **3**@C_{60} was shifted upfield from 42.5 ppm to 29.7 ppm. Such a shift indicates the effect of pyramidal inversion as well as the participation of the phosphine group in the complex formation. At 323 K, a sharp peak at −8 ppm was also observed similar to the free ligand **3** indicative of the temperature dependent partial reverse dissociation of **3**@C_{60} due to the inversion of **3** at the phosphorous atom.

The inclusion of C_{60} within the cavity created by the phosphine group of **3** was also further complemented with the dynamic ^1H NMR (Fig. 4). The broad singlet at 4.6 ppm of the methylene group of free triphosphine **3** at 297 K was shifted upfield to 3.95 ppm in the presence of C_{60}. The upfield shift of methylene peak was continued further upon increasing the temperature, which clearly indicates the effect of pyramidal inversion on the formation of inclusion of between C_{60} and **3**. At a higher temperature of 323 K, the methylene peak splits into two different peaks at 3.65 and 3.35 ppm due to the equilibrium observed between the complexed **3**@C_{60} and free triphosphine **3**. The pyramidal inversion of **3** is active in both uncomplexed and complexed conditions which can also be understood from the appearance of broad peaks for the aromatic protons between δ 8.1–6.8 ppm (Fig. S3). However, the aromatic proton peaks of free triphosphine **3** were shifted to the upfield region significantly with the rise in temperature indicating faster pyramidal inversion. But such a significant upfield shift of aromatic protons peaks of **3** was not observed after the addition of C_{60} attributed to the formation of **3**@C_{60} where the fullerene is expected to wrap within the tripodal cavity through multiple CH–π/π–π interactions.

To gain further insights into the structure of **3**@C_{60}, we performed the density functional theory (DFT) calculations by applying the B3LYP exchange–correlation functional with 6-31G* basis sets. All calculations were performed by using the Spartan'14

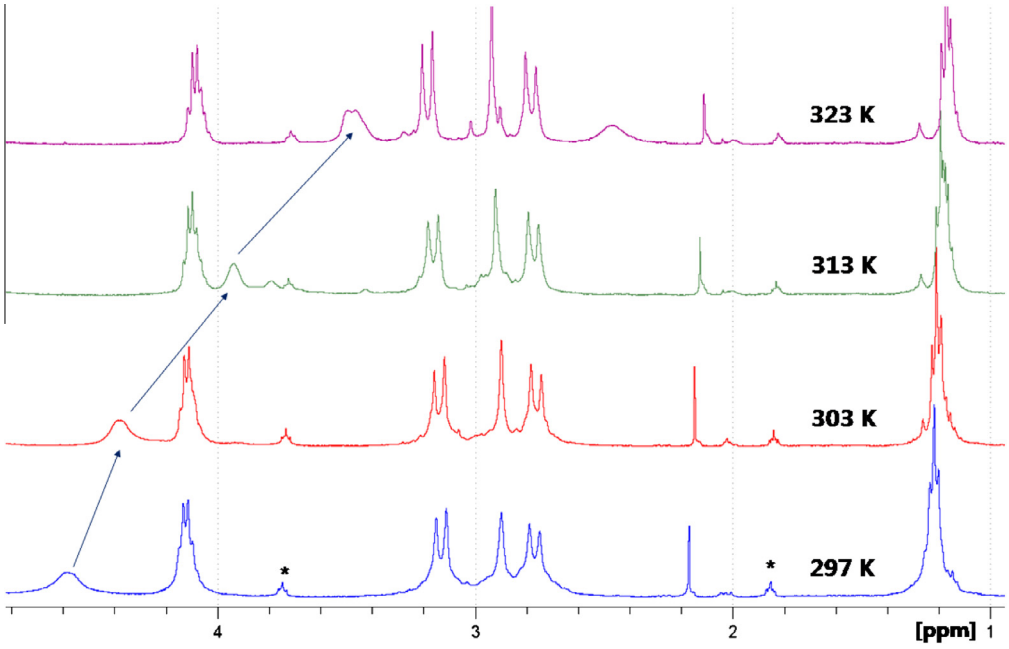

Figure 1. ^{1}H NMR spectra of **3** at various temperatures in $CDCl_3$ (*: THF).

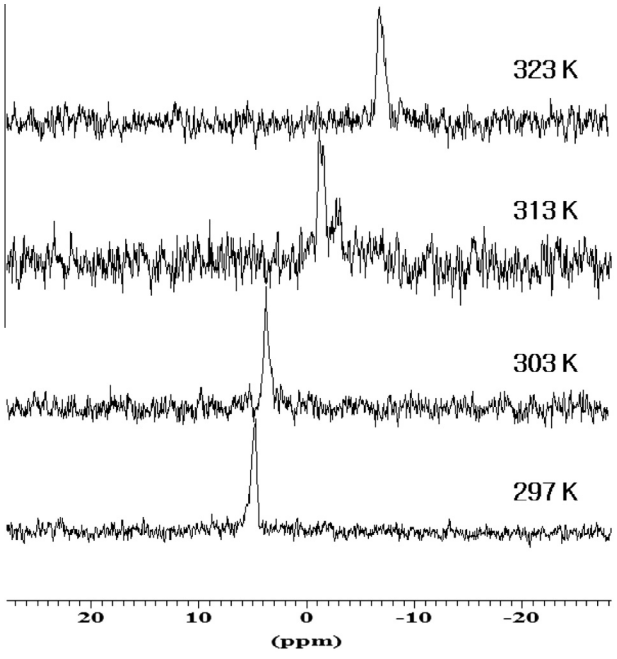

Figure 2. $^{31}P\{^{1}H\}$ NMR spectra of **3** at various temperatures in $CDCl_3$.

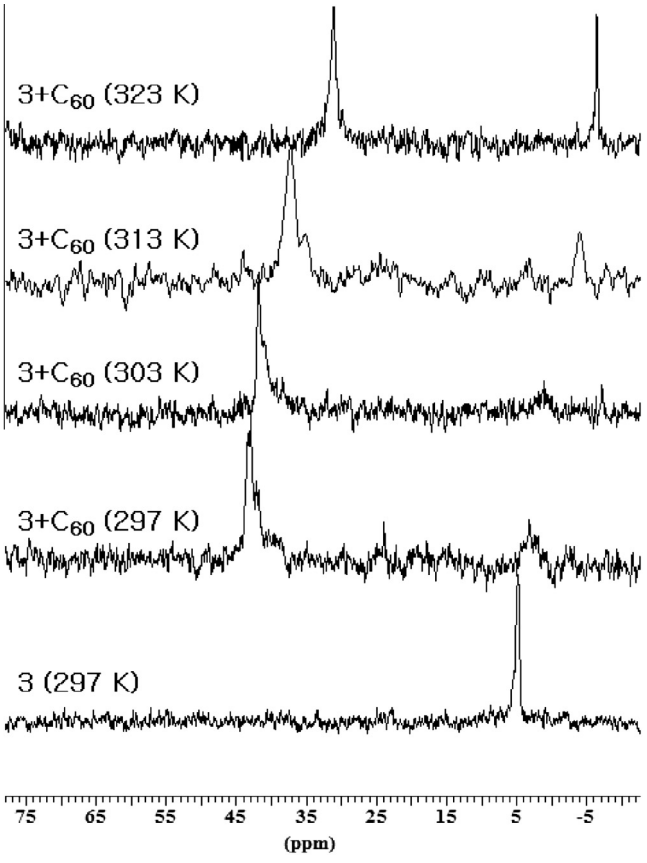

Figure 3. $^{31}P\{^{1}H\}$ NMR spectra of **3** (10 mM) with C_{60} at various temperatures (in $CDCl_3$).

software package. The energy minimized structure of **3** showed a C_{3v}-symmetry at the trindane framework, but the symmetry was distorted at the phosphine groups possibly due to the flexibility and/or the pyramidal inversion (Fig. 5a). Upon introduction of C_{60}, the three appended arms of **3** rearranged themselves to create a C_{3v}-symmetry tripodal cavity of diameter ~12.1 Å (Fig. 5b and c). It is well known that the size-fitting is the important factor for the formation of host–guest inclusion complex. The obtained diameter is close to the recommended diameter of 13 Å in order to host fullerenes like C_{60} or C_{70}.[18] Also, the computed **3**@C_{60} structure (Fig. 5) clearly supported the ability of **3** to recognize C_{60}.

The position of C_{60} within **3** was ascertained by analyzing the closest bond distances between the host and guest (Fig. 6a). The C_{60} was 3.632 Å above the plane of trindane platform whereas a distance of 3.891 Å was maintained from the trindane benzene

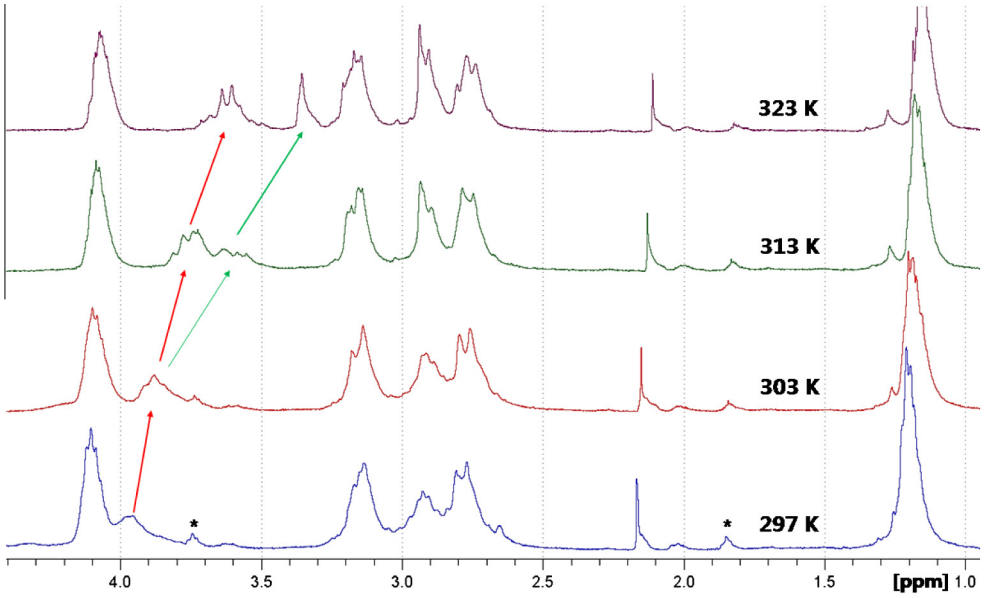

Figure 4. ^{1}H NMR spectra of **3** (10 mM) with C_{60} at various temperatures in $CDCl_3$ (*: THF).

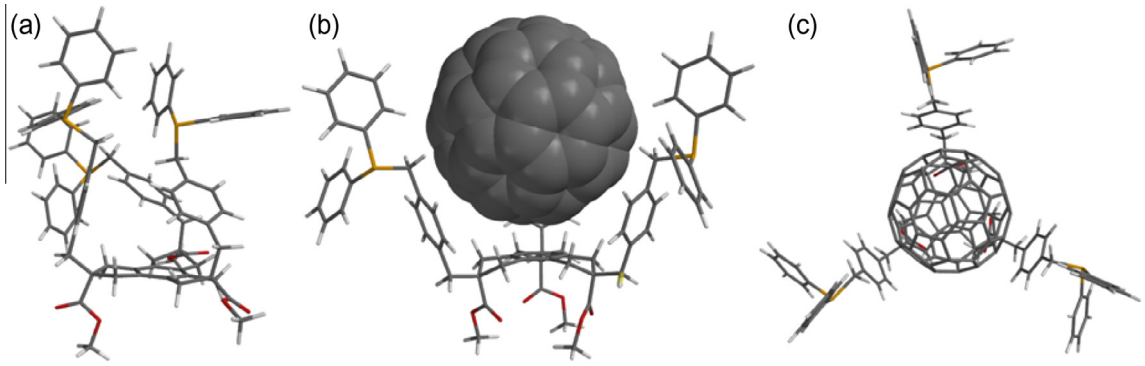

Figure 5. DFT (B3LYP/6-31G*) computed molecule structure of trisphosphine ligand **3** (a) and the two views of host–guest complex with **3**@C_{60} (b and c).

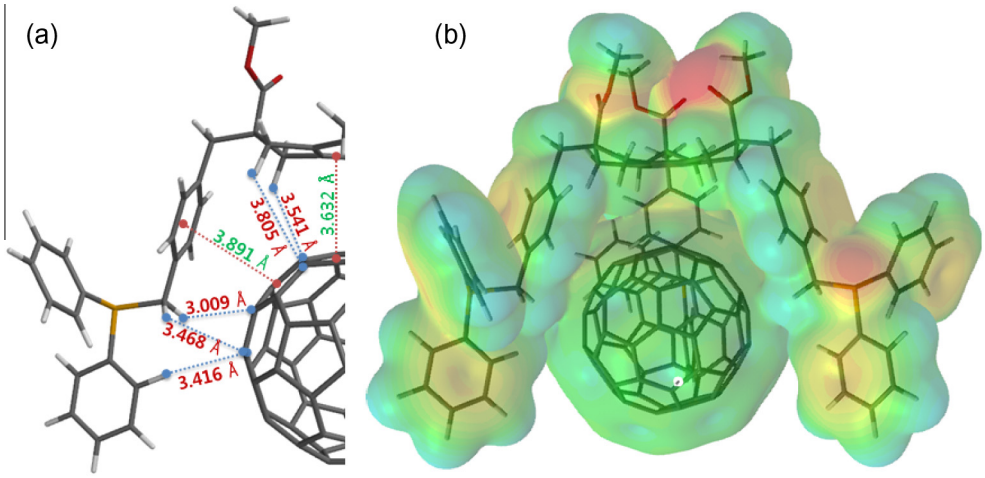

Figure 6. (a) Some important bond lengths and (b) the molecular electrostatic potential map (MEP) of **3**@C_{60}.

rings, which indicates that the guest C_{60} is located within the center of the host cavity. Also, the obtained distances are within the range for the possible π–π stacking interactions.[19] In addition, we also observed that the guest C_{60} wrapped with the help of fifteen CH–π interactions. These supramolecular interactions induced an internal charge transfer between C_{60} and **3**, which can be confirmed from the molecular electrostatic potential map (MEP)[20] of **3**@C_{60} (Fig. 6b).

Please cite this article in press as: Lim, D. S.; et al. *Tetrahedron Lett.* (2015), http://dx.doi.org/10.1016/j.tetlet.2015.08.069

In conclusion, we have introduced a novel trisphosphine ligand **3** derived from the rigid trindane tripodal framework in excellent yield. The structural characterization and pyramidal inversion of the trisphosphine ligand was discussed by ^{1}H NMR and ^{31}P NMR. Then, the catalytic activity of the ligand was applied in Pd-catalyzed Suzuki–Miyaura cross-coupling reaction of phenylboronic acid with 3-bromothiophene. The catalytic activity of **3** was found better than the mono-phosphine and di-phosphine ligands. The ^{31}P and ^{1}H NMR study inferred that the bowl shape with aromatic rings on the head showed the ability to encapsulate fullerene C_{60} through multiple CH–π/π–π interactions but partially decomplexed with the rise in temperature. Therefore, further study to develop capsular type stable supramolecular system with **3** is on the way considering the strong binding ability of phosphine toward various transition metal ions.

Supplementary data

Supplementary data associated with this article can be found, in the online version, at http://dx.doi.org/10.1016/j.tetlet.2015.08.069.

References and notes

1. Pascariu, A.; Iliescu, S.; Popa, A.; Ilia, G. J. *Organometal. Chem.* **2009**, *694*, 3982–4000.
2. Martin, R.; Buchwald, S. L. *Acc. Chem. Res.* **2008**, *41*, 1461–1473.
3. Wong, S. M.; So, C. M.; Chung, K. H.; Luk, C. H.; Lau, C. P.; Kwong, F. Y. *Tetrahedron Lett.* **2012**, *53*, 3754–3757.
4. Shi, J.-C.; Zhou, Z.; Zheng, S.; Zhang, Q.; Jia, L.; Lin, J. *Tetrahedron Lett.* **2014**, *55*, 2904–2907.
5. Gäbler, C.; Korb, M.; Schaarschmidt, D.; Speck, J. M.; Hilderbrandt, A.; Lang, H. *Chem. Comm.* **2015**, *54*, 96–99.
6. Pandiaranjan, D.; Ramesh, R.; Liu, Y.; Suresh, R. *Chem. Comm.* **2013**, *33*, 33–37.
7. Kondolff, I.; Feuerstein, M.; Doucet, H.; Santelli, M. *Tetrahedron* **2007**, *63*, 9514–9521.
8. Kang, P.-S.; Ko, S. B.; Ko, J. M.; Park, J. H. *Bull. Korean Chem. Soc.* **2009**, *30*, 2697–2700.
9. Schill, H.; de Meijere, A.; Yufit, D. S. *Org. Lett.* **2007**, *9*, 2617–2620.
10. Sygula, A.; Fronczek, F. R.; Sygula, R.; Rabideau, P. W.; Olmstead, M. M. *J. Am. Chem. Soc.* **2007**, *129*, 3842–3843.
11. Pérez, E. M.; Capodilupo, A. L.; Fernández, G.; Sánchez, L.; Viruela, P. M.; Viruela, R.; Ortí, E.; Bietti, M.; Martín, N. *Chem. Commun.* **2008**, 4567–4569.
12. Yanney, M.; Sygula, A. *Tetrahedron Lett.* **2013**, *54*, 2604–2607.
13. Fang, X.; Zhu, Y.-Z.; Zheng, J.-Y. *J. Org. Chem.* **2014**, *79*, 1184–1191.
14. Park, Y. S.; Kim, W.; Choi, H.-J. *Bull. Korean Chem. Soc.* **2014**, *35*, 3343–3345.
15. Choi, H.-J.; Park, Y. S.; Yun, S. H.; Kim, H.-S.; Cho, C. S.; Ko, K.; Ahn, K. H. *Org. Lett.* **2002**, *4*, 795–798.
16. Park, Y. S.; Bang, S.-H.; Choi, H.-J. *Tetrahedron Lett.* **2013**, *54*, 6708–6711.
17. Ruoff, R. S.; Tse, D. S.; Malhotra, R.; Lorents, D. C. *J. Phys. Chem.* **1993**, *97*, 3379–3383.
18. Bandow, S.; Takizawa, M.; Kato, H.; Okazaki, T.; Shinohara, H.; Iijima, S. *Chem. Phys. Lett.* **2001**, *347*, 23–28.
19. Yuan, K.; Zhou, C.-H.; Zhu, Y.-C.; Zhao, X. *Phys. Chem. Chem. Phys.* **2015**, *17*, 18802–18812.
20. The MEP was drawn by showing the most negative region by red color whereas the positive region by blue color, and then the color was extrapolated within red and blue to show the other regions.